Astron. Astrophys. 357, 429–436 (2000)

ASTRONOMY AND ASTROPHYSICS

X–ray variability and prediction of TeV emission in the HBL 1ES 1101–232

A. Wolter[1], **F. Tavecchio**[1], **A. Caccianiga**[2], **G. Ghisellini**[1], **and G. Tagliaferri**[1]

[1] Osservatorio Astronomico di Brera, Via Brera 28, 20121 Milano, Italy
[2] Observatorio Astronomico de Lisboa, Tapada da Ajuda, 1300 Lisboa, Portugal

Received 14 October 1999 / Accepted 11 February 2000

Abstract. 1ES 1101–232 is a bright BL Lac of the High frequency peak class. We present here the results of two *Beppo*SAX observations in which the source has shown a variation of about 30% in flux with a corresponding spectral variability. We interpret the overall spectral energy distribution in terms of an homogeneous SSC model and, by using also the TeV upper limit from a short Mark 6 pointing, derive constraints on the physical parameters of the source, in particular on the magnetic field strength. The overall Spectral Energy Distribution makes 1ES 1101–232 a very promising candidate for TeV detection.

Key words: galaxies: BL Lacertae objects: general – galaxies: BL Lacertae objects: individual: 1ES 1101-232 – X-rays: galaxies

1. Introduction

BL Lac objects form a minority class of active nuclei (see e.g. Urry & Padovani, 1995), but nevertheless their high luminosities and extreme variability in all bands make them an interesting subclass to study intrinsic properties of nuclear emission. Furthermore, the position of BL Lacs with respect to other active nuclei in the framework of Unification Models is a debated question. The current picture claims that BL Lacs are the fraction of Fanaroff-Riley I galaxies that point their jet towards us, but many details still need to be worked out. Often, BL Lacs are studied together with other classes of flat radio spectrum sources, to form the class of blazars.

Recently a sequence has been proposed for the subclass of gamma ray bright blazars, and possibly valid for all blazars, based on their bolometric luminosity (Ghisellini et al. 1998, Fossati et al. 1998). The overall spectral energy distribution has two peaks (in νF_ν representation), the one at lower energies due to synchrotron radiation and the higher energy one due to Inverse Compton scattering. It is proposed that the value of the peak frequency is the result of the balance between radiative cooling and acceleration of the corresponding electrons (see e.g. Ghisellini, 1999): in less luminous objects the radiative cooling is less efficient, allowing the accelerated electrons to reach higher energies. As a consequence, both the synchrotron and the inverse Compton peaks shift to higher frequencies as the bolometric intrinsic luminosity decreases. In this view, the class of BL Lacertae objects known as HBL (High frequency peak BL Lacs) has a smaller bolometric luminosity and a higher synchrotron peak frequency than the class of LBL (Low frequency peak BL Lacs). HBL are mostly found in X–ray selected samples, since they are expected to produce most of their synchrotron emission in the X–ray band. If the emission peak (as in the LBL objects) is at frequencies smaller than the observed X–ray band, the X–ray spectrum is steep (i.e. the steepening part above the peak), while HBL with a flat X–ray spectrum should have their peak in the observed X–ray band.

As part of a program aimed at a spectral survey of soft X–ray selected BL Lacs with *Beppo*SAX (Wolter et al. 1998), we have studied also 1ES 1101–232 (z=0.186), a bright BL Lac selected from the Slew Survey (Perlman et al. 1996) that shows an extreme behavior with a very flat X–ray spectrum. The object was detected, besides in the 0.1-10 keV energy band, also up to $\sim$ 100 keV in only ~ 6000 sec. The best fit of the source in the 0.1-100 keV band is given by a broken power law, with Galactic low energy absorption, that has a break energy E_0=1.36 (1.11–1.65) keV. The spectral slope (energy index) derived from the PDS is consistent with the one derived from the MECS above the break energy E_0: α_x = 1.03 (0.99–1.08) (Wolter et al. 1998).

We have constructed also the Spectral Energy Distribution (SED) for this object, using flux measurements collected from the literature, from radio to X–rays. We have fitted a cubic polynomial to the distribution in order to find the peak of the SED, that indeed falls in the *Beppo*SAX band ($\log \nu_{peak} \sim 17.48$, corresponding to ~ 1.3 keV). For this object, therefore, the break energy derived from the spectral fit in the X–ray band is consistent, albeit within its large indetermination, with the position of the synchrotron peak as derived from the overall distribution (SED).

The SED of 1ES 1101–232 is similar to that of the flaring state of Mkn 501 (Pian et al. 1998) and 1ES 2344+514 (Catanese et al. 1998; Giommi et al. 2000), and therefore we could expect a strong TeV emission. A quasi–simultaneous X–ray and TeV observation has been therefore scheduled, to confirm the X–ray spectrum of the source, and its overall shape, to detect possible variations in flux, that could constrain the physical parameters

Send offprint requests to: A. Wolter, (anna@brera.mi.astro.it)

of the source, and to monitor the TeV emission to search for possible detection.

The *Beppo*SAX data are presented here. The TeV observation, conducted in non–optimal weather condition, did not yield a detection, but we will use the upper limit (Chadwick et al. 1999a) to derive useful information on the physical mechanisms at work in this source. The plan of the paper is as follows: in Sect. 2 we describe the observational data obtained with *Beppo*SAX in the two epochs, in Sect. 3 we summarize the TeV predictions and observations, that help constraining the parameters of the source, by using the SED and theoretical models of emission as explained in Sect. 4. Sect. 5 presents our results and conclusions.

Throughout the paper a Hubble constant H_0=50 $\mathrm{km\,s^{-1}\,Mpc^{-1}}$ and a Friedman universe with a deceleration parameter q_0=0 are assumed.

2. *Beppo*SAX data

The X–ray astronomy satellite *Beppo*SAX is a project of the Italian Space Agency (ASI) with a participation of the Netherlands Agency for Aerospace Programs (NIVR). The scientific payload comprises four Narrow Field Instruments [NFI: Low Energy Concentrator Spectrometer (LECS), Medium Energy Concentrator Spectrometer (MECS), High Pressure Gas Scintillation Proportional Counter (HPGSPC), and Phoswich Detector System (PDS)], all pointing in the same direction, and two Wide Field Cameras (WFC), pointing in opposite directions perpendicular to the NFI common axis. A detailed description of the entire *Beppo*SAX mission can be found in Butler & Scarsi (1990) and Boella et al. (1997a).

The MECS consists of three equal units, each composed of a grazing incidence mirror unit and of a position sensitive gas scintillation proportional counter, with a field of view of 56 arcmin diameter, working range 1.3–10 keV, energy resolution $\sim 8\%$ and angular resolution ~ 0.7 arcmin (FWHM) at 6 keV. The effective area at 6 keV is 155 cm^2 (Boella et al. 1997b)

The LECS is a unit similar to the MECS, with a thinner window that grants a lower energy cut-off (sensitive in the energy range 0.1-10.0 keV) but also reduces the FOV to 37 arcmin diameter (Parmar et al. 1997). The LECS energy resolution is a factor ~ 2.4 better than that of the ROSAT PSPC ($\sim 32\%$ at 0.28 keV), while the effective area is smaller: 22 cm^2 at 0.28 and and 50 cm^2 at 6 keV.

The PDS is a system of four crystals, sensitive in the 13–200 keV band and mounted on a couple of rocking collimators, which points two units on the target and two units 3.5° aside respectively, to monitor the background. The position of the collimators flips every 96 seconds. Thanks to the stability of the instrumental background, the PDS has shown an unprecedented sensitivity in its energy range, allowing 3σ detection of $\alpha \sim 1$ sources as faint as 10 m Crab with 10 ks of effective exposure time (Guainazzi & Matteuzzi, 1997).

The source is not detected by the HPGSPC, so we will not discuss this instrument.

2.1. Observation of June 1998

The object has been observed in AO2 on 19 June 1998 for a total of 8958 sec (LECS – 3167 net counts); 24895 sec (MECS(2+3) – 10612 net counts) and 10792 sec (PDS on source – 1320 net counts). The AO2 observation has been performed with only 2 MECS (MECS2 and MECS3) since MECS1 was no longer active. The source has been observed almost in the same period (May 1998) by the Mark6 telescope (working in the GeV-TeV range).

The extraction of the *Beppo*SAX data has been performed with FTOOLS v4.0 and the spectral analysis with XSPEC v9.0, using the most recently available matrices (September 1997 release). The data analysis has been performed on the same guidelines as outlined by the *Beppo*SAX Cookbook (`http://www.sdc.asi.it/software/cookbook/`) and described e.g. in Wolter et al. (1998). We summarize here that counts are extracted in a circular region of 8.5'/4' (LECS/MECS) radius, and the background is taken from the blank sky images distributed by the *Beppo*SAX Data Center, in a region corresponding to the one used to extract source counts. Counts are binned so as to have at least 30 total counts in each bin to ensure applicability of the χ^2 statistics. Fit to LECS data are performed only up to 4 keV, as the response matrix of LECS is not well calibrated above this energy (see Orr et al. 1998). All confidence levels are computed using $\Delta\chi^2 = 2.7$ (corresponding to 90% for 1 interesting parameter), unless otherwise stated.

For the LECS+MECS combined data, a single power law is not acceptable ($> 3\sigma$) with $N_{\rm H}$ fixed at the Galactic value. If $N_{\rm H}$ is left free, the fit with a single power law is acceptable only at about 3σ (Prob $\sim 1.5\%$). The residuals are however skewed, showing that the fit is not good. The fit is significantly improved (F–test at $> 99.99\%$ probability) by using a broken power law shape. Results for the three models for LECS and MECS data are listed in Table 1.

For each observation, in the first fit (single power-law model with Galactic $N_{\rm H}$) we left the LECS normalization free with respect to the MECS normalization to account for the residual errors in intensity cross-calibration (see Cusumano, Mineo, Guainazzi et al. in preparation). The fitted value of 0.696 (1997) and 0.701 (1998) fall in the range expected given the current knowledge of the cross-calibration (F. Fiore, private communication; see also `http://www.sdc.asi.it/software/cookbook/cross_cal.html`). Since the ratio of the two normalizations depends on the position of the source in the detector, and not on the model chosen, we fix the LECS/MECS normalization to 0.7 also for the other subsequent models.

The PDS exposure time is not even twice than in AO1 (10.8 ks vs. 6.4 ks). Since the spectrum is steeper and the source is fainter than in the AO1 observation, the PDS detection is not more significant than the AO1 detection (2.6σ). In order to fit the PDS data alone we rebin them to 6 data points. We fix the absorbing column to the Galactic value ($N_H = 5.76 \times 10^{20}$ cm^{-2}) while the normalization with respect to the MECS and index are left free. The best fit slope is α_{PDS} = 1.02 [< 2.65], and

Table 1. Fit results for 1ES 1101–232 LECS+MECS data OBS. 19/06/98 **Low state**

Model	$N_{\rm H}^{a}$	α_1	α_2	E_0 keV	$F^{\rm b}$	$\chi^2(dof)$	Prob.
(1)	5.76	–	1.19(1.16-1.22)	–	2.60	267.1(195)	$< 0.5\%$
(2)	8.3(7.1-10.4)	–	1.25(1.22-1.29)	–	2.57	240.5(195)	1.5%
(3)	5.76	0.80(0.58-0.96)	1.29(1.25-1.33)	1.34(1.08-1.82)	2.55	216.2(194)	13%

(1) Single p.l., $N_{\rm H}$=$N_{\rm H}^{\rm Gal}$, LECS/MECS ratio free; (2) Single p.l., $N_{\rm H}$ free, LECS/MECS ratio=0.7; (3) Broken p.l., $N_{\rm H} = N_{\rm H}^{\rm Gal}$, LECS/MECS ratio = 0.7. Errors quoted are 90% confidence intervals.
[a] Column density in $\times 10^{20} {\rm cm}^{-2}$.
[b] Unabsorbed [2–10 keV] flux in 10^{-11} erg cm^{-2} s^{-1}.

Table 2. Fit results for 1ES 1101–232 LECS+MECS data OBS. 04/01/97 **High state**

Model	$N_{\rm H}^{\rm a}$	α_1	α_2	E_0 keV	$F^{\rm b}$	$\chi^2(dof)$	Prob.
(1)	5.76	–	0.97(0.95-1.00)	–	3.81	224.0 (182)	$< 2\%$
(2)	8.9(7.2-12.6)	–	1.03(0.99-1.08)	–	3.79	205.1 (182)	11%
(3)	5.76	0.59(0.35-0.74)	1.05(1.01-1.08)	1.36(1.11-1.65)	3.76	191.6 (181)	28%

(1) Single p.l., $N_{\rm H}$=$N_{\rm H}^{\rm Gal}$, LECS/MECS ratio free; (2) Single p.l., $N_{\rm H}$ free, LECS/MECS ratio=0.7; (3) Broken p.l., $N_{\rm H}$=$N_{\rm H}^{\rm Gal}$, LECS/MECS ratio = 0.7. Errors quoted are 90% confidence intervals.
[a] Column density in $\times 10^{20} {\rm cm}^{-2}$.
[b] Unabsorbed [2-10 keV] flux in 10^{-11} erg cm^{-2} s^{-1}.

the PDS/MECS ratio is 0.90, consistent with what is expected on the basis of cross-calibration of the instruments, with a χ^2 = 2.2(4 dof), for a probability of 70%, therefore statistically acceptable. However, given the low statistical significance of the PDS data, the uncertainty on the slope is high. We therefore fit the total spectrum, from 0.1 keV to ∼50 keV, using LECS, MECS and PDS data together: the result of the broken power law fit is shown in Fig. 1. It yields an unabsorbed flux in the [2–10 keV] band of $F_X = 2.54 \times 10^{-11}$ erg cm^{-2} s^{-1}, and a corresponding luminosity in the same band of $L_X = 4.7 \times 10^{45}$ erg s^{-1}. The PDS data are consistent with the LECS+MECS extrapolation.

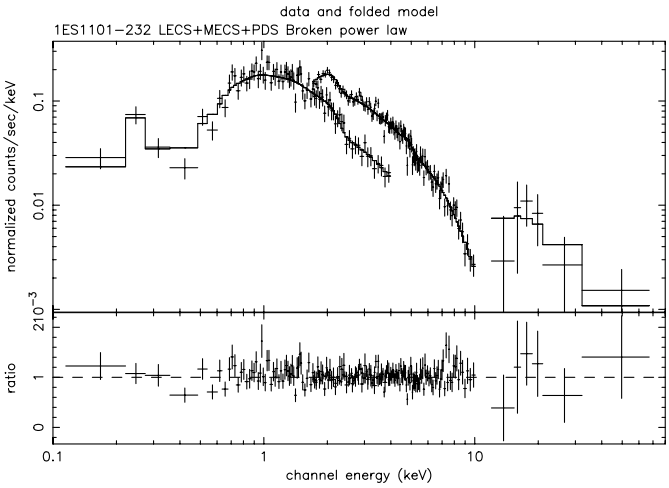

Fig. 1. X–ray spectrum (LECS+MECS+PDS) of June 1998, with broken power law fit (model 3 from Table 1)

2.2. Comparison of the 1997 and 1998 observations

For ease of comparison, we report in Table 2 the AO1 observation results of 1ES 1101–232, from Wolter et al. (1998). The LECS exposure was 5195 sec (2484 net counts), the MECS exposure was 13830 (9509 net counts) and the PDS on-source exposure was 6410 sec (1996 net counts). The best fit models of the LECS+MECS spectra for various spectral shapes are listed in Table 2, while in Fig. 2 the LECS+MECS+PDS spectrum is plotted, with the best fit of model (3).

In order to compare the two observations, we first check directly the count rates in the two epochs. The best representation is the ratio of the two observed spectra, that does not depend on the choice of models and parameters. We therefore bin the two spectra, the relative background and response matrices in 32 channels, in order to avoid having empty bins after background subtraction. We then divide the two background-subtracted count rates and plot the results (after having flagged out the energy ranges that are not well calibrated in the matrices) in Fig. 3. The ratio is consistent with being flat up to ~ 2 keV, and steepening after it, showing that a change in the spectrum occurred above ~ 2 keV. The two instruments, LECS and MECS, give a consistent ratio in the overlapping energy range. A fit with a constant in the interval 0.5–10 keV is not statistically acceptable.

Also comparing the fit results for the two observations of Jan 1997 and Jun 1998, we see that the high energy slope (α_2) is steeper in the second one. The flux, with all the three best

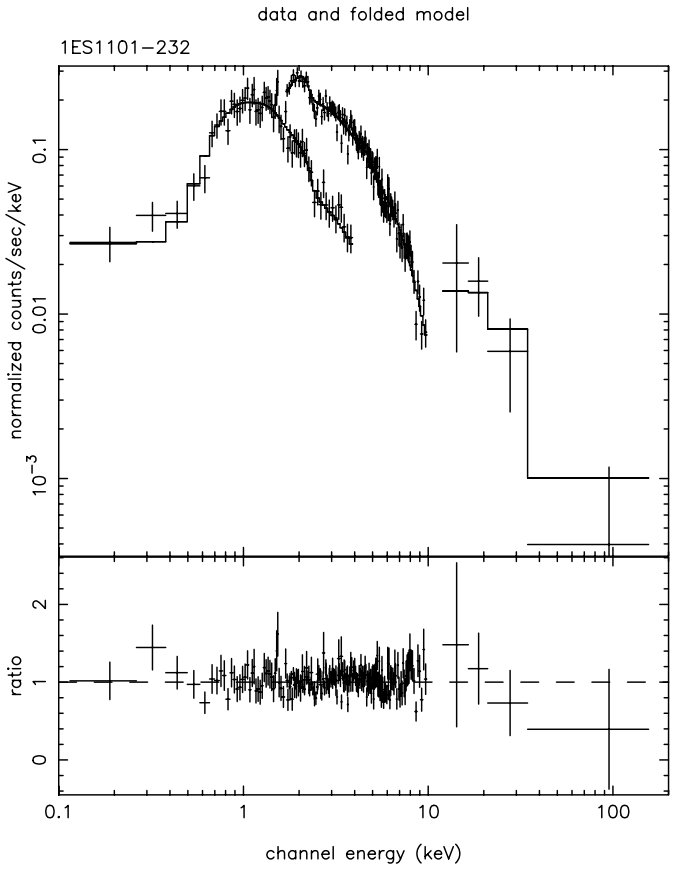

Fig. 2. X–ray spectrum (LECS+MECS+PDS) of Jan 1997, with broken power law fit (model 3 from Table 2).

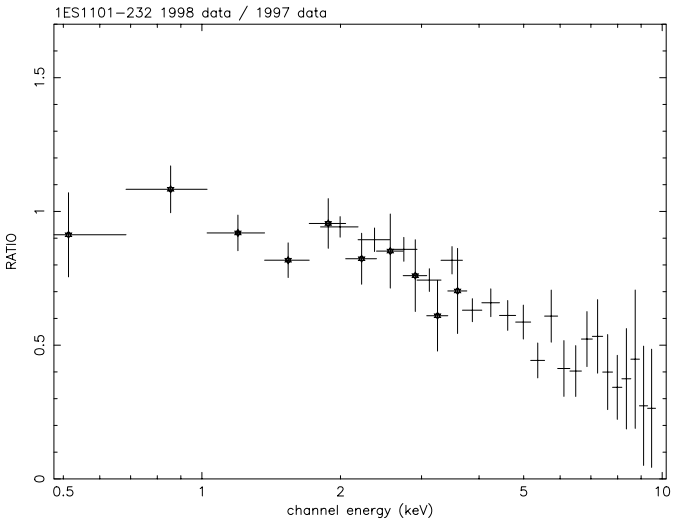

Fig. 3. Ratio of data point from the Jun 1998 and Jan 1997 observations. Stars indicate data points from the LECS instrument, crosses data points from the MECS instrument. The trend in the data, with a drop above $\sim$2 keV, is evident.

fit models reported in the tables, is a factor of $\sim$ 32% lower in the second than in the first one. The low energy slope (α_1) and the break energy (E_0) are instead consistent within the errors between the two observations.

We can make therefore the hypothesis that the different fluxes and spectra between the two epochs are explained by a change in the spectral slope above the peak of the synchrotron emission. Hence we fit all the data (1997+1998) simultaneously, keeping the low energy slope and break energy tied (equal one to each other, but free to vary) between the two observations. On the contrary, the high energy slopes in the two observations are left independent. The $N_{\rm H}$ is fixed to the galactic value, that fits well both observations. The PDS data are not used for the comparison, being of low statistical significance; the LECS and MECS data are re-binned to 100 total counts for each bin, to improve the significance of the individual data points, since no small range feature is present. The LECS/MECS normalization is again fixed to 0.7.

The resulting values of α_1 and E_0 are consistent with those of both single observations: α_1=0.72 [0.44, 0.88]; $E_0 = 1.17[0.93, 1.43]$ keV. The high energy slope is α_2^{1998} = 1.26 [1.19, 1.32], vs. α_2^{1997} = 1.01 [0.95, 1.07], confirming that the slope indeed steepened significantly. The χ^2 of the fit is 184.4 with 178 dof, corresponding to a probability of 36%. The errors quoted here are 90% confidence for 4 parameters of interest ($\Delta\chi^2 = 7.76$). The combined spectra (LECS and MECS) for both observations with the best fit model are shown in Fig. 4. We report in Table 3 the unabsorbed fluxes and rest-frame luminosities in the 0.1–2 and 2–10 keV bands for the two observations using the combined fit results.

The fluxes derived using the combined model are consistent with the fluxes derived from the two independent fits to the observations. We can therefore attribute the observed flux variation entirely to a steepening of the high energy (>2 keV) portion of the spectrum. There is no evidence, within the statistical uncertainties, of a change in α_1 or E_0, although in other well known sources (Mkn501, Mkn421, PKS2155–304) an increase in flux seems to be linked to an increase in E_0 and/or the high energy slope.

3. The TeV band

Blazars as a class have been shown to emit a large fraction of their power at high energies, in the MeV–TeV band. The current models assume that the high energy emission is produced by Inverse Compton scattering (e.g. the SSC model or the EC model, see Ghisellini et al. (1998) for the relevance of the two mechanisms), and the location of the peak of the Compton component depends mainly on the lower energy peak due to the Synchrotron component.

In particular, objects of the LBL kind, that have the synchrotron peak at soft energies, show their second peak at energies in the MeV–GeV range, and are in fact detected by EGRET on board CGRO (see Mukherjee et al. 1997). Objects of the HBL kind, that have their synchrotron peak at UV–X–ray frequencies, instead, should show the Compton peak in an even higher energy band. In fact, up to now, the only sources of VHE gamma rays (in the TeV band, by using Čerenkov detectors) are HBL: Mkn 421 (Punch et al. 1992), Mkn 501 (Quinn et al.

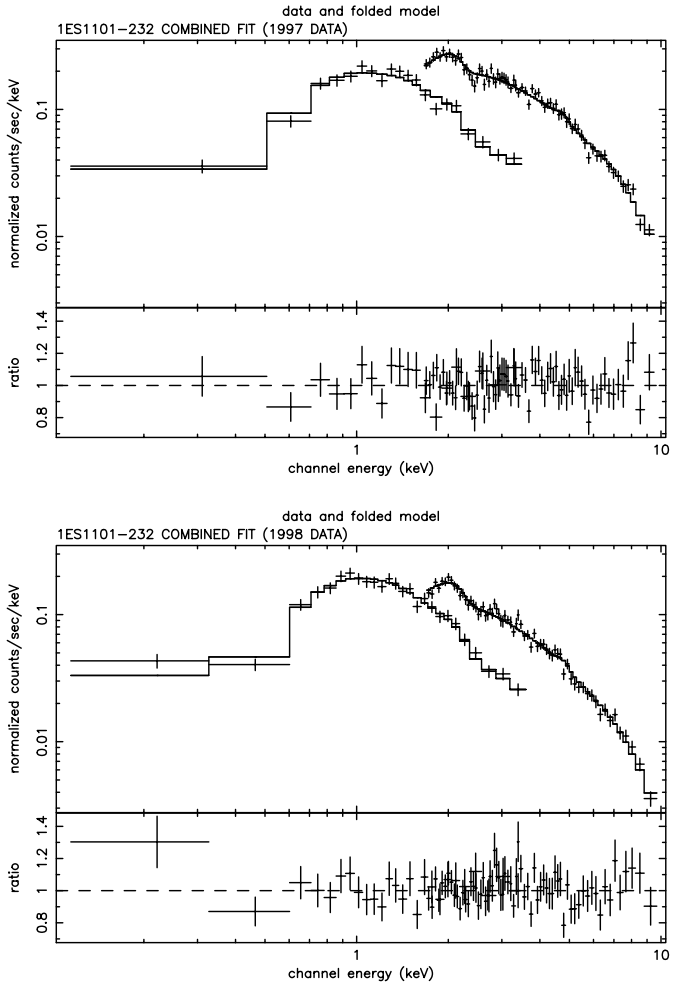

Fig. 4. LECS+MECS spectrum and broken power law fit for Jan 1997 (Upper Panel) and Jun 1998 (Lower Panel) observations. The broken power law fit of the two observations combined is given in the text.

1996), 1ES 2344+514 (Catanese et al. 1998), PKS 2155–304 (Chadwick et al. 1999b).

The new Čerenkov arrays allow the detection of bright sources in relatively short exposure times, and therefore it has been possible to monitor their variability: some of these objects have in fact shown periods of flaring activity on time-scales as short as 15 minutes (Gaidos et al. 1996, Aharonian et al. 1999).

Another point of debate is the amount of absorption of VHE photons due to the cosmic infra–red background. The aforementioned detected objects in fact are all nearby. Detection of sources that lie further away can therefore help in constraining the amount of the IR background (e.g. Stecker and De Jager, 1998).

The simultaneous detection of X–ray and TeV emission allows us to estimate a number of physical parameters of the source, such as the magnetic field and the Doppler factor (see e.g. Tavecchio et al. 1998). We will show in Sect. 4 that a number of interesting constraints can be derived also by using the upper limit derived in the TeV band, together with the X–ray band information.

Table 3. Unabsorbed Fluxes and Rest–Frame Luminosities for the two observations in the (0.1–2) and (2–10) keV energy bands.

Date	F[0.1-2]	F[2-10]	L[0.1-2]	L[2-10]
	$\times 10^{-11}$ erg cm^{-2} s^{-1}		$\times 10^{45}$ erg s^{-1}	
04/01/97	3.46	3.85	5.4	6.8
19/06/98	3.32	2.53	5.3	4.7

3.1. Predictions of TeV emission in 1ES 1101–232 from phenomenological constraints

A very simple prediction of the TeV emission can be made by following the scheme presented e.g. in Fossati et al. (1998). In this model a) the ratio of the frequencies of the high (Compton) and low (synchrotron) energy peaks is constant and equal to 5×10^8 and b) the high energy peak and the radio luminosity have a fixed ratio, $\frac{\nu_\gamma L_{peak,\gamma}}{\nu_{5GHz} L_{5GHz}} = 3 \times 10^3$. This model represents the average SED observed for the various classes, while single sources can deviate from this average phenomenological parameterization. This very simple relationship, however, allows us to make order of magnitude prediction even not knowing the physical conditions at the source. From the two expressions above we can derive both the expected frequency of the second peak and its intensity. The peak of the synchrotron emission is measured (this paper and Wolter et al. 1998) at $\nu_s = 3 \times 10^{17}$ Hz: the Compton peak is therefore expected at $\nu_C = 1.5 \times 10^{26}$ Hz which corresponds to $\sim$0.6 TeV. The measured radio flux at 5 GHz is 5×10^{-15} erg cm^{-2} s^{-1} (see references in Table 4). The expected flux at the Compton peak (0.6 TeV) is therefore $\sim 8. \times 10^{-12}$ photon cm^{-2} s^{-1}.

Another prediction can be made from the observed X–ray flux, by using the recipe of Stecker, De Jager & Salamon (1996). Within an SSC scenario they use simple scaling arguments to predict the TeV fluxes for HBL, based on the X–ray flux and the assumption that the properties of the emission are similar to those observed for Mkn 421. Their argument is partially supported by the actual detection of (a few) other sources for which they predicted possible detectability. The factor of increase between the synchrotron and Compton component is 10^9, and, assuming $L_C/L_s \sim 1$, they derive $\nu_{TeV} F_{TeV} \sim \nu_X F_X$. Therefore, from the observed X–ray properties for 1ES 1101–232 (peak around 1 keV and flux of 2.5–3.8 $\times 10^{-11}$ erg cm^{-2} s^{-1}), we infer that the expected Compton peak is around 1 TeV with a flux of 1.5–2.5×10^{-11} photon cm^{-2} s^{-1}.

These estimates make 1ES 1101–232 a good TeV candidate, at the border of current sensitivities, and possibly well above it during flaring activities.

3.2. TeV observations

1ES 1101–232 has been observed on the nights of 19–27 May 1998 with the Durham University Mark 6 atmospheric Čerenkov telescope. We summarize here the data analysis and the results presented in Chadwick et al. (1999a). The telescope uses the imaging technique to separate VHE gamma rays from

Table 4. References for the data points of Fig. 5.

Band	Reference
Radio 1.4GHz	NVSS: Condon et al. 1998 AJ 115, 1693
Radio 1.4GHz	Remillard et al. 1989 ApJ 345, 140
Radio 5 GHz	Perlman et al. 1996 ApJS 104, 251
Radio 5 GHz	Giommi et al. 1995 A&AS 109, 267
Optical V	Pesce et al. 1994 AJ 107, 494
Optical V	Lanzetta et al. 1995 ApJ 440, 435
Optical V	Giommi et al. 1995 A&AS 109, 267
Optical V	Jannuzi et al. 1994 ApJ 428, 130
Optical V	Falomo et al. 1994 ApJS 93, 125
IR J,H,K	Bersanelli et al. 1992 AJ 104, 28
IR K	Falomo et al. 1993 AJ 106, 11
UV 1400A	Pian & Treves 1993 ApJ 416, 130
UV 1400A	Edelson et al. 1992 ApJS 83, 1
X–ray 2 keV	Perlman et al. 1996 ApJS 104, 251
X–ray 2 keV	Giommi et al. 1995 A&AS 109, 267
EGRET	Fichtel et al. 1994 ApJS 94, 551

the cosmic ray background, together with a robust noise-free trigger (Armstrong et al. 1999). Data are taken in 15 minutes segments, alternating ON-source with an equal number of OFF-source observations. After removal of cloud–affected data, there are a total of 10.5 hours ON-source data and the same amount of OFF-source data. Data are screened for "good" events by the selection criteria listed in Table 2 of Chadwick et al. (1999a). The source was not detected and an upper limit of F_{TeV} [> 300 GeV] = 3.7×10^{-11} photons cm^{-2} s^{-1} has been derived.

The data have been investigated for time variability on time-scales of days (at a flux limit of $\sim 1\times10^{-10}$ cm^{-2} s^{-1}) and 15 min intervals. There is no evidence for any bursting behavior (Chadwick, private communication).

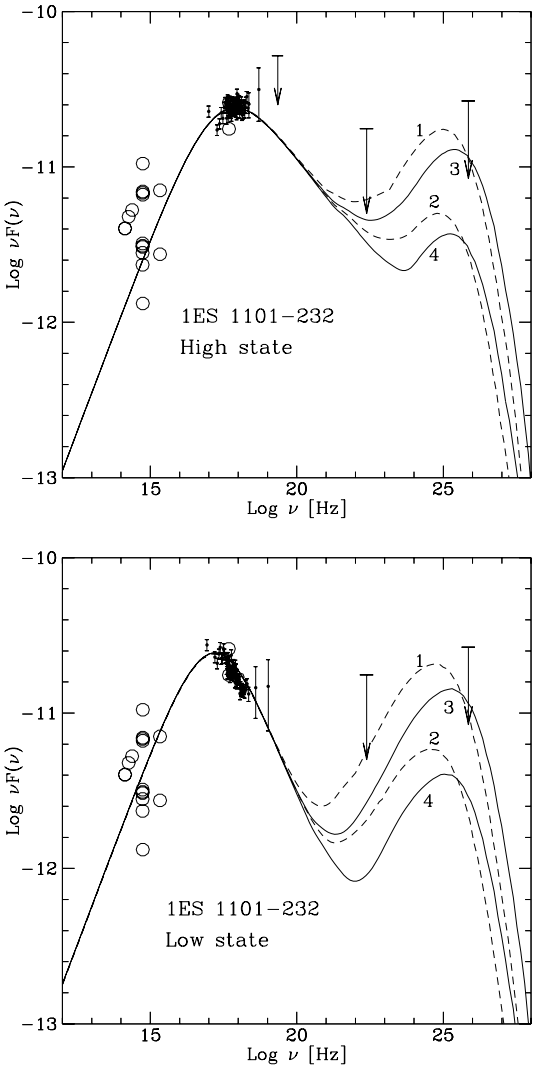

Fig. 5. SED of the two *Beppo*SAX epoch observations *Top:* 04/01/97 – high state; *Bottom:* 19/06/98 – low state, plus models. Large empty circles represent historical data from literature, while arrows indicate upper limits from EGRET (MeV) and Mark6 (GeV-TeV) experiments respectively (see Table 4 for references). Small dots with error-bars are the unfolded X–ray spectra discussed in this work. Lines represent the spectra computed with the SSC model (see text for details) with different model parameters, reported in Table 5: dashed lines represent spectra calculated with $\delta = 10$ and two different values for the magnetic field B; similarly, solid lines represent spectra calculated with $\delta = 20$ and two different values for the magnetic field B.

4. SED construction and TeV predictions from theoretical models

We have constructed the overall Spectral Energy Distribution (SED), using both data from literature and the *Beppo*SAX spectra from the two observations. We construct two different SED, one for each *Beppo*SAX observation, that are clearly modeled by a different synchrotron state. The two SED are presented in Fig. 5.

We have reproduced the SED in both X–ray states with a simple homogeneous SSC model. The source is modeled as a spherical region with size R, uniform and tangled magnetic field B, in motion toward the observer with a bulk Lorentz factor Γ. The region is filled by a population of relativistic electrons with a distribution of Lorentz factors given by: $N(\gamma) = K\gamma^{-n_1}(1+\gamma/\gamma_b)^{n_1-n_2}$, where the asymptotic slopes are n_1 and n_2, the break point is γ_b and K is a normalization factor. The self–Compton emission is derived taking into account the full Klein–Nishina (KN) cross section, computed using the relations reported in Jones (1968; see also Blumenthal & Gould 1970). We do not take into account absorption of IR photons by the infrared background, whose emission level is still uncertain. This implies that in principle the derived curves are upper limits to the detectable VHE emission, also because the redshift of 1ES 1101–232 is only slightly smaller than the limit ($z = 0.2$) chosen to monitor blazar emission in the TeV band by the HEGRA experiment (Rhode & Meyer, 1997). On the other hand, a detection of the source in this band would provide also a measure of the density of IR background photons.

Although the complete determination of the set of physical parameters for the SSC model requires the knowledge of the positions of both the synchrotron peak and the Inverse Compton

Table 5. Input parameters for the models of Fig. 5

High State							
#	δ	B (G)	γ_b $\times 10^4$	R cm	K cm^{-3}	n_1	n_2
1	10	0.3	15.8	1×10^{16}	1.7×10^4	2	3.5
2	10	0.6	11.2	1×10^{16}	5.9×10^4	2	3.5
3	20	0.1	19.3	1×10^{16}	7.9×10^3	2	3.5
4	20	0.2	13.5	1×10^{16}	2.8×10^4	2	3.5
Low State							
#	δ	B (G)	γ_b $\times 10^4$	R cm	K cm^{-3}	n_1	n_2
1	10	0.5	8.45	1×10^{16}	2.5×10^4	2	3.9
2	10	1.0	5.98	1×10^{16}	8.9×10^3	2	3.9
3	20	0.1	13.3	1×10^{16}	6.3×10^3	2	3.9
4	20	0.2	9.40	1×10^{16}	2.2×10^3	2	3.9

peak (as discussed in Tavecchio et al. 1998), we can put strong constraints to the parameters using the information provided by the X–ray spectrum and the TeV upper limit suggesting that the condition $L_C/L_s \leq 1$ applies.

We note here that the analytical relations discussed in Tavecchio et al. (1998) in the KN regime are obtained with a step approximation for the KN cross–section. In the extreme KN regime the numerical values given by this approximation might differ from the results of the numerical model derived with the full KN treatment, but we can use the analytical discussion as a guideline for the numerical model.

Typical variability time-scales observed in HBLs ($t_{var} \sim 10^{3-4}$ s, see e.g Zhang et al. 2000, Giommi et al. 1999, 2000) suggest Doppler factors δ in the range 10–20 and sizes of $R \leq 10^{16}$ cm. We fixed the radius to $R = 10^{16}$ cm. This choice directly puts a lower limit to the value of the magnetic field:

$$B\delta^{2+\alpha_1} > A \times (1+z)^{\alpha_1} \left[\frac{g}{\nu_c \nu_s}\right]^{(1-\alpha_1)/2} \left(\frac{L_s}{t_{var} L_C^{1/2}}\right) \qquad (1)$$

where $g(\alpha_1, \alpha_2)$ is a constant related to the spectral indices α_1 and α_2 and A is the appropriate constant (see Tavecchio et al. 1998 for details on (1)). From this relation we can infer that an upper limit on L_C and an estimate of t_{var} directly puts a lower limit for B. The physical reason for this lower limit is related to the fact that the synchrotron peak Luminosity is proportional to the product $N_e B^2$ (where N_e is the number of emitting electrons), while the ratio between the Compton peak Luminosity and the synchrotron peak Luminosity is proportional to N_e: therefore an upper limit to L_C/L_s gives an upper limit to N_e and this, together with the synchrotron Luminosity, provides the lower limit for the magnetic field B. Another way of describing the effect, assuming that the scattering is in the Thomson regime, is that in this case requiring $L_C/L_s < 1$ corresponds to require that the ratio between the synchrotron and the magnetic energy densities $U_s/U_B < 1$. For a given source size and Doppler factor the synchrotron radiation energy density is fixed, and the above relation then corresponds to a lower limit on the value of the magnetic field.

In Fig. 5 we plot the spectrum of both states computed for two different values of δ ($\delta = 10$ for the dashed lines, $\delta = 20$ for the solid lines), and for two different values of the magnetic field B, as listed in Table 5. The lowest value of B has been determined by requiring not to over-produce the high energy (TeV) emission, since, for a given synchrotron luminosity, size and Doppler factor, the ratio between the self Compton and the synchrotron powers depends only on the magnetic field.

We take this value, listed in Table 5, for the models 1 and 3 shown in Fig. 5. For models 2 and 4 we have doubled the B value, and decreased the relativistic electron density and γ_b accordingly, in order to produce the same amount of synchrotron flux and about the same synchrotron peak frequency. In this case the self–Compton flux decreases, due to the decreased electron density.

The transition from the high to the low state is consistent with a change of the second slope n_2 and with a decrease of γ_b by a factor of 1.5–2. This behavior is similar to what observed in the other well known TeV BL Lac, such as PKS 2155–304 (see e.g. Chiappetti et al. 1999), Mkn 501 (e.g. Pian et al 1998) and Mkn 421 (Maraschi et al. 1999), where high X-ray states are interpreted as states with either higher γ_b and/or higher magnetic field.

It is evident from Fig. 5 that a small change in the magnetic field, while still consistent with the X–ray (*Beppo*SAX) observations, produces a dramatically different amount of TeV photons. Assuming that the size of the source and the Doppler factor do not vary substantially with time, variations of the synchrotron flux can be attributed to changes of the density of electrons and/or the magnetic field. If this is the case, we expect that the TeV emission can be easily detected, either for X–ray fluxes slightly brighter than what observed up to now, or by longer TeV exposure times.

5. Results and conclusions

The X–ray spectrum of 1ES 1101–232 as measured by *Beppo*SAX is fitted only by a broken power law (a single power law or an absorbed power law are not statistically acceptable) with a break at 1.3 - 1.9 keV. From the first to the second observation, the spectrum varied at high energies, becoming softer (steeper). The flux decrease, by about 32%, has occurred in the 2–10 keV band. The PDS observation are not of statistical significance sufficient to put a real constraint on the spectrum.

Even if the variation in the X–ray band is not dramatic, we can clearly distinguish between the two states, that are modeled by different parameters of the synchrotron component.

By using the TeV upper limit and the two *Beppo*SAX observations we model also the higher energy portion of the spectrum as a self–Compton component, by using the model described e.g. in Tavecchio et al. (1998) that assumes a simple homogeneous SSC model in the KN regime, in which the relativistic electrons have a broken power law energy distribution.

The two X-ray states of the source are described by varying this distribution, assuming that the other relevant parameters (R and δ) are nearly constant.

We can compare these results with what found for the few TeV detected sources. The choice of Doppler factor of 10 and 20 made here is in the interval of the values of δ found by other authors for Mkn 421, PKS2155–304 and Mkn501, that range from $\delta \sim 5$ (e.g. Takahashi, 1999; Mkn 421, Catanese et al. 1998: Mkn 501) to $\delta \sim 30$ (e.g. Bednarek & Protheroe 1999: Mkn501; Kataoka et al 2000: PKS2155–304; Bednarek & Protheroe 1997: Mkn 421). At the same time, values of B in excess of 0.03 G and up to 1 G (Chiappetti et al. 1999) are found for the same sources.

Of the three above mentioned objects, the most similar to 1ES 1101–232 is Mkn 501, for which different measures have been produced: e.g. $\delta \geq 15$ & $B = 0.8$G (Pian et al. 1998); $\delta = 15$ & $B = 0.2$G (Kataoka et al. 1999); $\delta = 30$ & $B = 0.7$G (Bednarek & Protheroe 1999), in good agreement with the values of Table 5.

Even if based, besides the accurate X-ray spectral determination up to ~ 50 keV, only on a TeV upper limit we can infer that the physical conditions in 1ES 1101–232 are similar to the brightest TeV sources, making it a very promising candidate for TeV observations, and a testbed for the SSC model. Furthermore, since the redshift of 1ES 1101–232 is intermediate, a detection of this source in the VHE range would pose constraints on the density of the IR background photons that is still at the moment very uncertain.

Acknowledgements. This work has received partial financial support from the Italian Space Agency. We would like to thank Paula Chadwick and S.J. McQueen for informing us about their VHE results in advance of publication, Paolo Giommi and Roberto Della Ceca for helpful discussion and comments, and an anonymous referee for useful suggestions that improved the readability of the paper.

References

Aharonian F.A., Akherperjanian A.G., Berrio J.A., et al., 1999, A&A 341, 69
Armstrong P., Chadwick P.M., Cottle P.J., et al., 1999, Experimental Astronomy vol. 9, 51
Bednarek W., Protheroe R.J., 1997, MNRAS 290, 139
Bednarek W., Protheroe R.J., 1999, MNRAS 310, 577
Blumenthal, Gould, 1970, Rev. of Modern Phys. 42, 237
Boella G., Butler R.C., Perola G.C., et al., 1997a, A&AS 122, 299
Boella G., Chiappetti L., Conti G., et al., 1997b, A&AS 122, 327
Butler C., Scarsi L., 1990, SPIE 1344, 46
Catanese M., Akerlof C.W., Badran H.M., et al., 1998, ApJ 501, 616
Chadwick P.M., Lyons K., McComb T.J.L., et al., 1999a, ApJ 521, 547
Chadwick P.M., Lyons K., McComb T.J.L., et al., 1999b, ApJ 513, 161
Chiappetti L., Maraschi L., Tavecchio F., et al., 1999, ApJ 521, 552
Fossati G., Maraschi L., Celotti A., Comastri A., Ghisellini G., 1998, MNRAS 299, 433
Gaidos J.A., Akerlof C.W., Biller S.D., et al, 1996, Nat 383, 319
Ghisellini G., 1999, In: Takalo L. (ed.) The BL Lac Phenomenon. ASP conf. ser. 159, 311
Ghisellini G., Celotti A., Fossati G., Maraschi L., Comastri A., 1998, MNRAS 301, 451
Giommi P., Padovani P., Perlman E., 2000, MNRAS in press, astro-ph/9907377
Giommi P., Massaro E., Chiapetti L., et al., 1999, A&A 51, 59
Guainazzi M., Matteuzzi A., 1997, SDC-TR 011
Jones, 1968, Phys. Rev 167, 1159
Kataoka J., Takahashi T., Makino F., et al., 2000, ApJ 528, 243
Kataoka J., Mattox J.R., Quinn J., et al., 1999, ApJ 514, 138
Maraschi L., Fossati G., Tavecchio F., et al., 1999, ApJ 526, L81
Mukherjee R., Bertsch D.L., Bloom S.D., et al., 1997, ApJ 490, 116
Orr A., Parmar A.N., Yaqoob T, Guainazzi M., 1998, In: Scarsi L., Bradt H., Giommi P., Fiore F. (eds.) Nuclear Physics B Proceedings Supplements, Elsevier Science B.V
Parmar A.N., Martin D.D.E., Bavdaz M., et al., 1997, A&AS 122, 309
Perlman E.S., Stocke J.T., Schachter J.F., et al., 1996, ApJS 104, 251
Pian E., Vacanti G., Tagliaferri G., et al., 1998, ApJ 492, L17
Punch M., Akerlof C.W., Cawley M.F., et al., 1992, Nat 358, 477
Quinn J., Akerlof C.W., Biller S., et al., ApJ 1996, 456, L83
Rhode W., Meyer H., 1997, In: Proceedings of the International Conference on: Relativistic Jets in AGNs. p. 223
Stecker F.W., De Jager O.C., Salamon M.H., 1996, ApJ 473, L75
Stecker F.W., De Jager O.C., 1998, A&A 334, L85
Takahashi T., Madejski G., Kubo H., 1999, Astropart. Phys. 11, 173
Tavecchio F., Maraschi L., Ghisellini G., 1998, ApJ 509, 608
Urry C. M., Padovani P., 1995, PASP 107, 803
Wolter A., Comastri A., Ghisellini G., et al., 1998, A&A 335, 899
Zhang Y.H., Celotti A., Treves A., et al., 1999, ApJ 527, 719